Ultrasonics Sonochemistry 37 (2017) 405–413

Contents lists available at ScienceDirect

Ultrasonics Sonochemistry

journal homepage: www.elsevier.com/locate/ultson

Effect of ultrasound on the interaction between (−)-epicatechin gallate and bovine serum albumin in a model wine

Qing-An Zhang [a,*], Xi-Zhe Fu [a], Juan Francisco García Martín [b]

[a] Lab. of Food & Physical Field Processing, School of Food Engineering and Nutrition Science, Shaanxi Normal University, Xi'an, 710119 Shaanxi Province, PR China
[b] Department of Chemical Engineering, Faculty of Chemistry, University of Seville, 41012 Seville, Spain

ARTICLE INFO

Article history:
Received 12 September 2016
Received in revised form 20 January 2017
Accepted 20 January 2017
Available online 30 January 2017

Keywords:
Ultrasound
Interaction
Bovine serum albumin
(−)-Epicatechin gallate
Model wine

ABSTRACT

Ultrasound is considered as a potential novel technique for improving the quality of some wines. In this paper, a model wine firstly was constructed with the standards of (−)-epicatechin gallate (ECG) and bovine serum albumin (BSA) as target compounds. Then, the experiments were conducted to investigate the effect of ultrasonic irradiation on the binding properties between ECG and BSA including quenching mechanism, binding parameters, binding forces, energy transfer distance and conformational changes determined by spectral analysis. The results indicate that ultrasound definitely has some regular effects on the binding interaction of BSA and ECG, and can induced the conformation variation of BSA in the simulated wine, which may suggest that the ultrasound might be employed to modify the wine organoleptic property by regulating the interaction between phenolic compounds and proteins from the autolysis of yeasts, since they are similar to the standards of ECG and BSA, respectively.

1. Introduction

Wine aging is an important procedure to obtain high quality wine, during which complicated reactions were involved among sugars, organic acids, phenols and yeast autolysis products, subsequently modifying the organoleptic properties of wine such as astringency, bitterness and off-odour [1,2]. During aging, on the one hand, monomeric flavonoids slowly combine with each other together with procyanidins to generate polymers, which accounts for the formation of coloration and specific flavour in white or red wine [3–5]. On the other hand, yeasts, one of the main constituents of lees (the residue formed at the bottom of vats of wine during storage after fermentation), undergo autolysis triggered by their own hydrolytic enzymes, and subsequently release the intracellular constituents including proteins, polysaccharides and other low molecular weight products [6–8]. As a result, the wine is enriched by compounds released from yeast cell, which have been developed to promote red wine sensory characteristics, such as astringency, texture, colour and mouth-feel, due to their affinity to the polyphenols in red wine. That is, to some extent, the organoleptic characteristics of wine can be adjusted or improved by influence the interaction between those compounds obtained from yeast cell and phenols in wine. [9–11].

Among these compounds derived from yeasts, much lower affinity exist between polyphenols and polysaccharides [12], while the binding effects of the protein to phenols play a comparatively more important role in the wine sensory. In the previous research, it has been demonstrated that yeast proteins can adsorb phenolic compounds [13,14], precipitate or bind with polyphenols, during which the colour stability can be improved and astringency of the wine can be reduced [15,16]. In addition, yeasts proteins play important roles in unique flavour and foaming properties for wine, especially sparkling wine [17], which could be modified by the interaction between the proteins and phenols in wine. Therefore, it is significant to investigate the mechanisms of interactions between proteins and phenols in wine system (pH = 3.8, 12% (v/v) ethanol), which is still controversial and demands a further research [13,14].

Although natural aging in oak barrels is a traditional and reliable method to produce high-quality wine, this method is high-cost, time-consuming and labour-intensive. In order to overcome these defects above-mentioned in natural aging, some novel techniques have been reported including addition of oak chips, aging on lees, and the utility of different emerging physical methods [18,19]. In comparison, among all those physical techniques studied, ultrasound, a relatively low-cost, non-hazardous and eco-friendly technique, which has been widely applied in the field of food processing, is regarded as one of the considerably promising technology to obtain high-quality wines in a shorter time [18,20–

* Corresponding author.
E-mail address: qinganzhang@snnu.edu.cn (Q.-A. Zhang).

http://dx.doi.org/10.1016/j.ultsonch.2017.01.031
1350-4177/

22]. Some researchers have proposed the potential of ultrasound for accelerating the aging of several kinds of wines, such as rice wine and rice alcoholic beverage [23,24]. Masuzawa, Ohdaira and Ide [25] had illustrated that a soft ultrasonic treatment could lead to an increase of phenols in red wine, and subsequently could be of assistance to accelerate wine maturation. Our previous studies have also revealed that the ultrasonic frequency and exposure time significantly affected the concentration of total phenolic compounds and electrical conductivity of red wine [1,2]. Furthermore, ultrasonic irradiation can also induce the generation of 1-hydroxyethyl radicals in red wine and a model wine [26], which is thought as an initiator for the complex reactions during wine aging. Overall, given the effects of ultrasound on modifying the wine properties, it can be expected that the interaction between proteins and phenolic compounds in wine might be influenced or even regulated by ultrasonic irradiation.

However, previous research mainly focused on the changes of physicochemical properties and macroscopic parameters of wine under different ultrasonic conditions. There is still a lack of studies concerning the changing mechanisms of wine organoleptic property from the interaction between phenols and proteins, which is initiated by ultrasonic irradiation. The aim of this study was therefore performed to investigate the interaction between proteins and phenolic compounds in wine by analysing the effect of ultrasound on the quenching mechanism, binding parameters, binding forces, energy transfer distance and conformational changes, and the final purpose is to promote the application of ultrasound in accelerating wine aging. Considering the complexity of the phenolic compounds and yeast proteins involved in wine, ECG, as a typical monomeric phenol in wine, and BSA, a common and soluble protein, were selected to simulate the corresponding components. Moreover, ultrasonic frequency was set as a critical parameter investigated due to its significant influence on chemical reactions [26,27].

2. Materials and methods

2.1. Materials

BSA was purchased from Sigma-Aldrich Chemicals Company (USA). ECG was purchased from Chengdu Must Bio-technology Co., Ltd, China. The double-distilled water was used throughout the experiment. Other reagents were of analytical grade.

2.2. Model wine preparation

ECG was directly dissolved in 12% (v/v) ethanol solution and then the pH was adjusted to 3.8 with tartaric acid to simulate a model wine solution, which was freshly prepared in order to avoid being oxidized. Similarly, BSA was also dissolved in the tartaric acid solution (pH = 3.8) contained with ethanol (12%).

2.3. Fluorescence measurement

The samples at different temperatures (288, 298 and 308 K) and frequencies (25, 40 and 59 kHz, 298 K) were performed in F-7000 fluorescence spectrophotometer (Hitachi, Japan) equipped with a 1.0 cm quartz cell and a thermostatic bath. For each experimental group treated with ultrasonic irradiation or not, the BSA concentration was kept at 1.0×10^{-6} mol·L^{-1}, while the concentration of ECG varied from 0 to 4.0×10^{-6} mol·L^{-1} at regular intervals. The excitation and emission slit width was set to 2.5 nm. The excitation wavelength was set at 280 nm (excitation of the tryptophan (Trp) and tyrosine (Tyr)), and the emission spectra were recorded from 290 to 450 nm at a scan rate of 1200 nm·min^{-1}. The synchronous fluorescence spectra were measured from 265 to 350 nm ($\Delta\lambda$ = 15 nm) and from 240 to 350 nm ($\Delta\lambda$ = 60 nm), respectively. Appropriate blanks corresponding to the model wine solution (without BSA or ECG) were employed to subtract the fluorescence background.

2.4. Analysis of fluorescence quenching between ECG and BSA

In order to investigate the fluorescence quenching mechanism between ECG and BSA, the following equations and parameters were used. To be specific, fluorescence quenching is described by the Stern-Volmer equation [28–31]:

$$\frac{F_0}{F} = 1 + k_q \tau_0 [Q] = 1 + K_{SV}[Q] \quad (1)$$

where F_0 and F denote the fluorescence intensities in the absence and presence of quencher, respectively. K_{SV} is the Stern-Volmer quenching constant; K_q is the bimolecular quenching rate constant; τ_0 is the average lifetime of the molecular fluorescence in the absence of quencher, which is around 10^{-8} s; [Q] is the concentration of the quencher. Therefore, Eq. (1) was applied to determine K_{SV} by linear regression of a plot of F_0/F against [Q].

Furthermore, the temperature-dependent thermodynamic parameters including free energy changes (ΔG^0), enthalpy changes (ΔH^0) and entropy changes (ΔS^0) can be studied on the basis of the following equations (Eqs. (2)–(4)), if the ΔH^0 does not vary significantly within a certain temperature range [32,33]:

$$\Delta G^0 = -RT \ln K_b \quad (2)$$

$$\ln \frac{K_2}{K_1} = \left[\frac{1}{T_1} - \frac{1}{T_2}\right] \frac{\Delta H^0}{R} \quad (3)$$

$$\Delta G^0 = \Delta H^0 - T\Delta S^0 \quad (4)$$

where R is the gas constant, T stands for the experimental temperature, K_b (Eq. (2)) refers to the binding constant at the corresponding temperature, K_1 and K_2 (Eq. (3)) are the binding constants corresponding to the temperature of T_1 and T_2, respectively.

Moreover, binding parameters, which is very useful to investigate the binding effect of small molecules with proteins, can be determined by the following equation [32]:

$$\log\left[\frac{F_0 - F}{F}\right] = n \log K_b + n \log \frac{1}{[Q] - \frac{(F_0 - F)[P]}{F_0}} \quad (5)$$

where F_0 and F are the fluorescence intensities before and after the addition of the quencher, respectively; K_b is the binding constant and n is the average number of binding sites per protein molecule; [P] and [Q] are total protein concentration and total quencher concentration, respectively. Plots of $\log(F_0-F)/F$ against $\log(1/([Q]-[P](F_0-F)/F_0))$ are utilized to determine the values of K_b and n from the intercept and the slope, respectively.

As for the energy transfer, based on the Förster theory [31,34], the transfer efficiency is defined as follows:

$$E = \frac{R_0^6}{R_0^6 + r^6} = 1 - \frac{F}{F_0} \quad (6)$$

where E can be determined experimentally from the donor fluorescence in the presence (F) and absence (F_0) of the quencher, standardized to the same concentration of the donor; r is the donor-to-acceptor distance, and R_0 is the critical distance when the efficiency of transfer is 50%.

$$R_0^6 = 8.79 \times 10^{-25} K^2 n^{-4} \phi J \quad (7)$$

In Eq. (7), K^2 stands for the orientation factor, n is the refracted index of medium and φ refers to the fluorescence quantum yield of the donor. In this research, K^2 = 2/3, n = 1.36 and φ = 0.118 [35]. J is

the overlap integral which expresses the degree of spectral overlap between the donor emission and the acceptor absorption, and can be calculated from the following equation:

$$J = \frac{\int_0^\infty F(\lambda)\varepsilon(\lambda)\lambda^4 d\lambda}{\int_0^\infty F(\lambda)d\lambda} \quad (8)$$

where F(λ) is the corrected fluorescence intensity of the donor at wavelength λ, and ε(λ) is the molar absorption coefficient of the acceptor at the wavelength λ.

2.5. Measurement of UV–Vis spectra about ECG and BSA

UV–Vis spectra were recorded from 195 to 450 nm with a TU-1810 spectrophotometer (PERSEE Analytical Instrument Ltd., Beijing, China) equipped with a 1.0 cm quartz cell.

2.6. Circular dichroism (CD) measurement of BSA

The CD spectra of BSA solution in the absence or presence of ECG with different ultrasonic treatment were recorded in the range of 200–260 nm at 298 K by the Chirascan CD spectroscopy instrument (Applied Photophysics Ltd., UK) with a 1 mm cell. The concentration of BSA was kept at 1.0×10^{-6} mol·L^{-1} and the molar ratios of ECG to BSA were varied from 0:1 to 2:1. The corresponding contribution of the model wine solution to the spectra was recorded and digitally subtracted to the spectra at the same ultrasonic conditions. The compositions of the secondary structure on free proteins and ECG-binded complex were estimated according to the CD spectra [33].

2.7. Effect of ultrasonic treatment on the interaction between BSA and ECG

Experiments were carried out in an ultrasonic bath (SB-500 DTY, Ningbo Scientz Biotechnology Co., Ltd, China), which can work at the frequencies of 25, 40 and 59 kHz with a variable power output. Ultrasonic energy was transferred from the bottom to the medium within the bath by ten transducers and the maximum power was 500 W. The temperature was maintained constant during treatment by means of Xiangya DLSB-5/20 circulation pump of closed-loop cryogenic refrigerator (Shanghai, China). Different ultrasonic frequencies, namely 25, 40 and 59 kHz, were employed to investigate its effect on the binding interaction between BSA and ECG with the total electric power of 500 W for 30 min at the temperature of 298 K, and its affecting mechanism was analysed by the above-mentioned parameters. It should be noted that even though the power of ultrasonic bath was set to 500 W, only a part of the total electric power could be transferred into ultrasonic power (ultrasonic wave form), among which a large portion of the ultrasonic wave would be reflected on the surface of the vessel or weakened by the material of vessel. Therefore, this total electric power was selected in order to clearly present the modification of the interaction initiated by ultrasound. All the experiments were performed in duplicates.

3. Results and discussion

3.1. Effect of ultrasound frequency on the fluorescence quenching spectra between ECG and BSA

As can be observed in Fig. 1, the fluorescence intensity of BSA decreased with the increasing of ECG concentration in the model wine with or without ultrasonic irradiation. A characteristic fluorescence emission spectrum of BSA is displayed with a maximum value at the wavelength of 336 nm, which is mainly attributed to

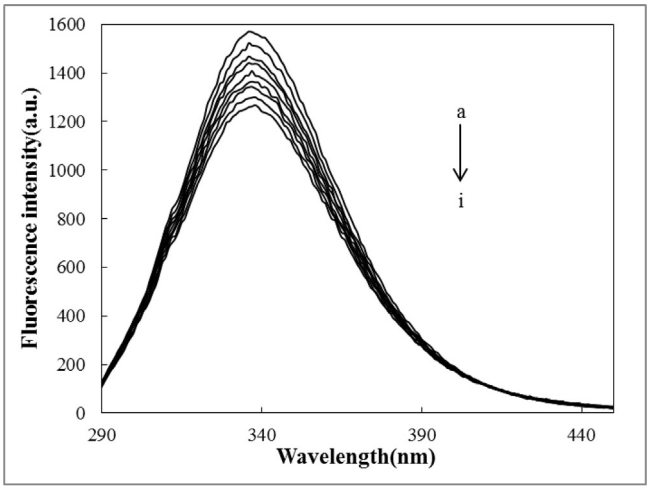

(a)

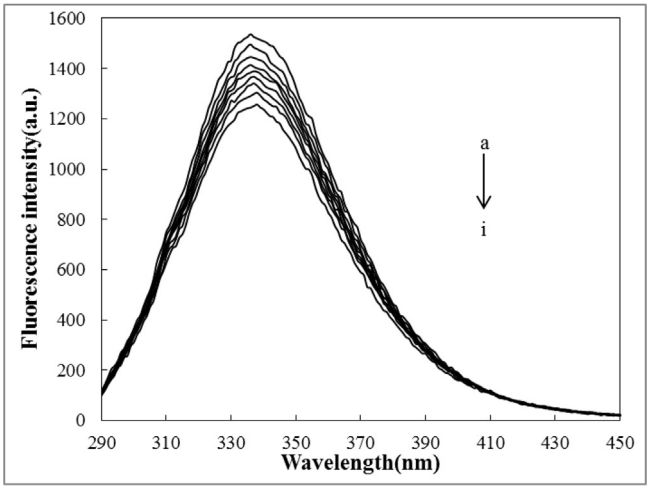

(b)

Fig. 1. Emission spectra of BSA (1.0×10^{-6} mol·L^{-1}) in the presence of different concentrations of ECG (a–i: 0, 0.5, 1.0, 1.5, 2.0, 2.5, 3.0, 3.5 and 4.0, 10^{-6} mol·L^{-1}) at 298 K and pH = 3.8. (a) without ultrasound irradiation; (b) with ultrasound irradiation of 59 kHz, 500 W and 30 min.

the tryptophan (Trp) residues [34]. By comparing the two top curves (fluorescence spectra) in Fig. 1a and b, only very little difference exist between them, while the curves decreased significantly with the increasing concentration of ECG. Similarly, only extremely limited difference can be observed when comparing the fluorescence data obtained from the samples including BSA solely treated with ultrasound at three different frequencies with untreated ones (data not shown). Therefore, these results indicate that ECG plays a major role in the fluorescence quenching process under the experimental condition. Although previous studies suggested that the fluorescence of Trp would be destroyed by intensive ultrasound [36], comparatively mild ultrasonic irradiation provided by ultrasonic bath preserved fluorescence signal of BSA well in the experimental condition, which would be attributed to scattered ultrasonic wave energy throughout the whole bath and the energy loss throughout the ultrasound wave propagation, especially energy reflection on the surface of the vessel and energy decline by the vessel material.

Besides, with increasing ECG additions, a slightly upward shift of the wavelength could be observed, which may indicate that the ECG can interact with BSA and quench its fluorescence together

with the conformational changes of BSA in the model wine even after ultrasonic irradiation, and ultrasonic treatment could hardly overwhelm the change of immediate environment of the tryptophan residues induced by ECG. However, comparatively, it should be noted that a general narrowed range or extent of fluorescence quenching after ultrasonic irradiation might convey an intriguing signal that ultrasound may play a considerable role in interaction between ECG and BSA in the wine-like solution. Moreover, as the ultrasonic frequency increases, the general range or extent of fluorescence quenching declines (data not shown), which demonstrates that fluorescence quenching capacity of ECG on BSA may get weaker as receiving ultrasonic irradiation of higher frequency, and a regular effect was triggered by different frequency of ultrasound irradiation on the interaction between ECG and BSA in model wine. Due to the defects of rough information provided by fluorescence quenching spectra, the quenching mechanism, binding parameters and other information are therefore required to explain the effect of different ultrasound frequency on the interaction of BSA and ECG in wine-like solution, which will be discussed in the following section.

3.2. Mechanism of fluorescence quenching and the effects of ultrasound frequency

The Stern-Volmer plots and the corresponding K_{SV} values were shown and listed in Fig. 2 and Table 1, respectively. In the studied conditions, a linear Stern-Volmer plot is observed, which may mean only one type of quenching mechanism occurring (static or dynamic). Generally, the dynamic and static quenching can be distinguished by their different dependence on the temperature. For the dynamic quenching, higher temperature leads to faster diffusion and larger amounts of collisional quenching. The quenching constant increases with the temperature rising, while the opposite effect would be observed for the static quenching [28]. As shown in Table 1, the K_{SV} values present a decline trend with the increasing of temperature, and the k_q values are much greater than 2×10^{10} - $L \cdot mol^{-1} \cdot s^{-1}$ which is the limiting diffusion rate constant of the biomolecule [37]. Therefore, we can conclude that the quenching mechanism belongs to the static quenching.

In comparison, the quenching constants decrease with the increasing of ultrasound frequency employed (Fig. 2b, Table 1b). Considering the static quenching mechanism, that is, the fluorescence is mainly initiated by formation of the ECG-BSA complex. Furthermore, the decreasing values of quenching constants imply a receding stability for the complex. The results observed in Fig. 2b and Table 1b can be attributed to the acoustic cavitation, which produces cavitation bubbles as well as the collapse of the cavity, and subsequently causes locally instant high pressures and temperatures, creating an extreme environment affecting the stability of the generated complex between ECG and BSA. Generally, an increased ultrasonic frequency would result in smaller bubbles. Being size-dependent, the bubble burst occurs along with the downsizing of the bubble size distribution. The burst of a smaller bubble gives a higher amount of energy, and such phenomena possibly do much contribution to the decreased stability of the complex with higher frequencies. Moreover, bubbles undergo nonlinear oscillations under the influencing of ultrasound, and the vibration would be quicker with the increasing of frequency. Consequently, the quicker vibration may have a negative effect on the stability of the complex generated by ECG and BSA in the model wine solution.

3.3. Thermodynamic parameters and the interacting force between ECG and BSA in model wine

The interaction forces between small molecules and macromolecules mainly include the electrostatic interaction, multiple hydrogen bonds, van der Waals force and hydrophobic force [29,33]. The signs and magnitudes of the thermodynamic parameters can account for the main forces involved in the interaction, which can provide some basic information of the binding process and contribute to a better understanding for the effect of ultrasound on the interaction between BSA and ECG in the model wine.

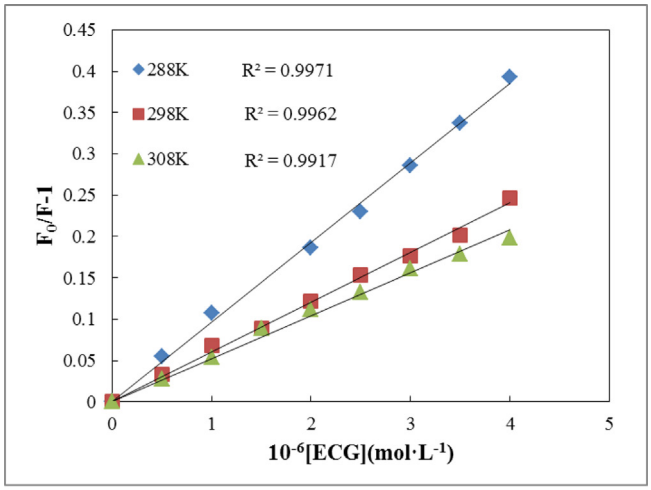

(a)

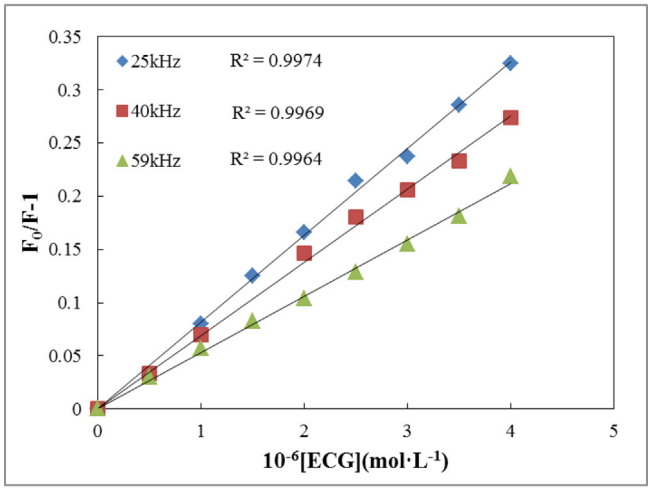

(b)

Fig. 2. Stern-Volmer plots for the quenching of BSA by ECG in the model wine. (a) at different temperatures; (b) with different ultrasound frequency at 298 K, 500 W and 30 min.

Table 1
Stern-Volmer quenching constants for the ECG-BSA system, (a) at different temperatures without ultrasound; (b) with different ultrasound frequency.

Table 1a Stern-Volmer quenching constants for the ECG-BSA system at different temperatures

T (K)	K_{SV} (10^4 L mol^{-1})	K_q (10^{12} L mol^{-1} s^{-1})	R^2
288	9.620	9.620	0.9971
298	6.009	6.009	0.9962
308	5.198	5.198	0.9917

Table 1b Stern-Volmer quenching constants for the ECG-BSA system induced by ultrasonic treatment at 298 K

Frequency (kHz)	K_{SV} (10^4 L mol^{-1})	K_q (10^{12} L mol^{-1} s^{-1})	R^2
25	8.162	8.162	0.9974
40	6.883	6.883	0.9969
59	5.289	5.289	0.9964

It can be observed in Table 2a that the binding of ECG to BSA in the model wine is an exothermic process accompanied by the values of positive ΔS^0 and negative ΔG^0. The binding process is therefore spontaneous based on the negative values of ΔG^0. The positive entropy probably accounts for hydrophobic interaction, and the negative enthalpy may derive from electrostatic interactions [38]. However, owning to the relatively acidic condition used here, the contribution of the electrostatic interaction to association process, in general, would be limited as little charge existed on phenols for experimental pH, and, therefore, more importance should be attached to hydrophobic interaction. In addition, according to the thermodynamic laws summed up by Ross and Subramanian [39], van der Waals interaction and hydrogen bond may also make negative contribution to the enthalpy. Considering the structure of the ECG, especially the galloyl group, each galloyl group provides three hydroxyl groups and a benzene ring, which can establish hydrogen and hydrophobic bonds, respectively, increasing the binding affinity to BSA.

3.4. Effect of ultrasound frequency on the binding parameters between ECG and BSA

Binding parameters are very useful to investigate the binding effect of small molecules with proteins. The results for the binding process with ultrasonic irradiation in the model wine were shown in Fig. 3b and Table 2c, whereas the data for the binding process in the absence of ultrasonic treatment was demonstrated in Fig. 3a and Table 2b. The correlation coefficients are higher than 0.99, indicating the interaction between ECG and BSA fits well to Eq. (5). Therefore, the binding parameters can be calculated according to Eq. (5).

From Fig. 3a and Table 2b, it can be observed that the binding constant (K_b) decreased with the temperature increasing, indicating that the increasing temperature raises the diffusion coefficient of the system, and consequently leads to a weaker binding effect, which is consistent with the results of static quenching. From Table 2c and Fig. 3b, an interesting declining trend of the binding constant (K_b) can be observed when the ultrasound frequency increased at a constant ultrasonic temperature of 298 K, which implies that the higher ultrasound frequency plays a negative role

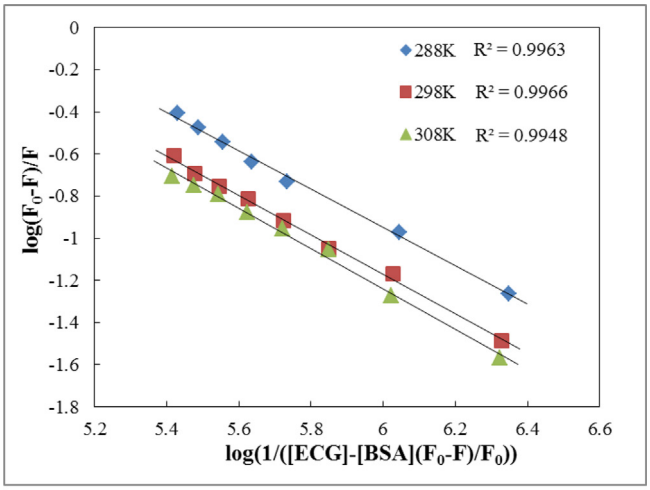

(a)

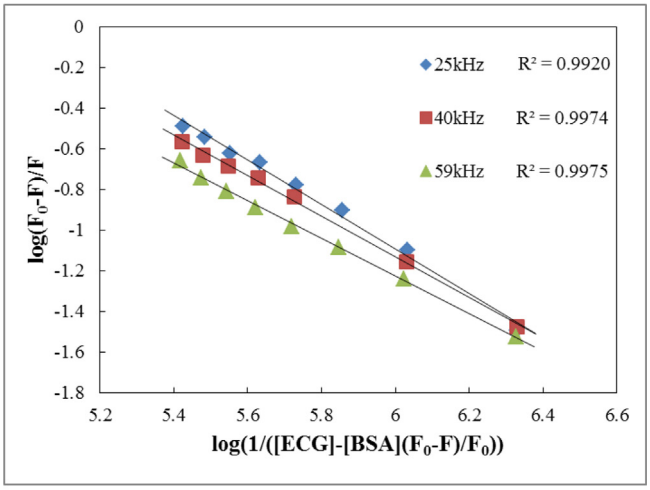

(b)

Fig. 3. Double-log plots for BSA quenched by ECG in the model wine. (a) at different temperatures; (b) with different ultrasound frequency at 298 K, 500 W and 30 min.

Table 2
Thermodynamic parameters and binding parameters for the ECG-BSA system, (a) thermodynamic parameters at different temperatures; (b) binding parameters at different temperatures without ultrasound; and (c) binding parameters with different ultrasound frequency at 298 K.

Table 2a Thermodynamic parameters for the ECG-BSA system at different temperatures

T (K)	ΔH (kJ mol^{-1})	ΔG (kJ mol^{-1})	ΔS (kJ mol^{-1})
288	−21.617	−27.350	0.020
298		−27.084	0.018
308		−27.748	0.020

Table 2b Binding parameters for the ECG-BSA system at different temperatures

T (K)	K_b (L mol^{-1})	n	R^2
288	9.135×10^4	0.9112	0.9963
298	5.593×10^4	0.9343	0.9966
308	5.083×10^4	0.9575	0.9948

Table 2c Binding parameters for the ECG-BSA system induced by ultrasonic treatment at 298 K

Frequency (kHz)	K_b (L mol^{-1})	n	R^2
25	9.995×10^4	1.0908	0.9920
40	7.343×10^4	0.9974	0.9974
59	4.707×10^4	0.9234	0.9975

in the binding process. This result may be directly derived from the nonlinear oscillations of the cavitation bubbles, because higher ultrasound frequency means more rapid oscillation of the microbubbles and, therefore, increases the frequency of intermolecular collision, which could disrupt the weak acting force and reduce the stability of the ECG-BSA complex. In addition, higher frequency would lead to, in general, smaller bubbles, and owning to the energy released from the burst bubble is size-dependent, the burst of smaller bubbles would provide a higher amount of energy, which would also do much negative contribution to the stability of the complex. Moreover, the higher frequency of the pressure/temperature pulse in the microenvironment generated by the collapse of the cavity could enhance diffusion coefficient, and subsequently have a negative effect on the stability of the complex, which is consistent with the results obtained from the temperature increasing process. Furthermore, the higher ultrasound frequency could lead to an increase of free radicals, especially 1-hydroxyethyl radicals identified in our previous studies [26], and the radicals may interact with ECG around the bubble-liquid interface, and hence result in a competition with the binding interaction, which may interfere or disrupt the binding process. In addition, compared with the binding constant derived from the model system without ultrasound irradiation, the relatively higher binding constants (K_b) obtained from the ultrasonic treatment of

25 kHz and 40 kHz indicate that lower frequency ultrasonic irradiation may promote or facilitate the binding process between the ECG and BSA. These results may be attributed to the increasing possibility of intermolecular collision initiated by ultrasound cavitation, hence promoting the binding process, and, meanwhile, the negative effects on binding interaction are relatively minor at lower ultrasound frequency. As for the binding sites number, the values of n are roughly equal to 1 in all conditions, implicating that there is only one suitable site of BSA to form the ECG-BSA complex and the binding interaction is exclusive to 1:1 (BSA: ECG) whether ultrasound was involved or not. The declining trend of the n with the increasing frequency, apart from the reasons existing in the binding constants decreasing, may be attributed to the conformational changes in BSA triggered by ultrasonic cavitation, and hence change the accessibility of ECG to the binding sites. Generally, the effect of ultrasound cavitation could be reduced at higher frequency due to the insufficient negative pressure to produce cavitation during rarefaction period or insufficient time for the collapse of bubbles during compression period. However, given the relative low ultrasound frequencies assayed, a cycle of the ultrasonic wave in each frequency assayed provides enough time for the enlargement, compression and ultimately collapse of the bubbles. Thus, the negative effects of higher frequency on the cavitation phenomenon are relatively limited, and only play a minor role in the binding interaction at the studied situation.

Theoretically, more free radicals derived from higher ultrasound frequency could accelerate the wine aging process, however, the negative effect of higher frequency on the binding interaction between ECG and BSA would not improve the quality of wine. Hence, it is significant to elaborate the mechanism of ultrasonic effects and select a suitable lower frequency for a specific wine to make the advantage of ultrasound, as reported by Chang [24] and Zheng [40].

3.5. Effect of ultrasound frequency on the energy transfer between BSA and ECG

Energy transfer measurement has been widely used to estimate the distances between sites (a donor and an acceptor) on macromolecules and the effects of conformational changes on these distances [31]. In light of the Eqs. (6)–(8), the overlap integrals and critical distance at different temperatures and different ultrasound frequencies were listed in Table 3.

As shown in Table 3a and b, the values of r (the critical distance) were lower than 8 nm in all conditions, which indicates that the energy transfer from the BSA to ECG occurs with high possibility. The larger values of r with the temperature rising depicted in Table 3a implicate that the increasing temperature could enlarge the distance between the donor and the acceptor, which may be attributed to the lager diffusion coefficient generated by higher temperature hence moving the sites further apart. From Table 3b, it can be observed that the r value increases with ultrasound frequency rising at a constant temperature of 298 K, indicating that ultrasound with higher frequency could result in a farther distance between the donor and the acceptor. Apart from the lager diffusion coefficient and the quicker nonlinear oscillations of the cavitation bubbles provoked by higher ultrasound frequency, more energy released from smaller bubbles initiated by higher ultrasonic frequencies would also contribute to the disruption of hydrophobic interaction and hydrogen bond, which would result in the conformational change of the complex and, therefore, enlarge the distance between the donor and acceptor. Furthermore, the r value of the sample treated at the ultrasound frequency of 25 kHz is smaller than that of untreated one, implicating that lower frequency may increase the binding affinity between ECG and BSA in the model wine, which is consistent with the results derived from binding parameters.

Table 3
Overlap integrals and the critical distance for the ECG-BSA system, (a) at different temperatures without ultrasound; (b) with different ultrasound frequency at 298 K.

Table 3a Overlap integrals and the critical distance at different temperatures

T (K)	J (cm^3 L mol^{-1})	R_0 (nm)	r (nm)
288	8.4916×10^{-15}	2.35	3.41
298	8.4930×10^{-15}	2.35	3.68
308	8.4879×10^{-15}	2.35	3.83

Table 3b Overlap integrals and the critical distance with different ultrasound frequencies at 298 K

Frequency (kHz)	J (cm^3 L mol^{-1})	R_0 (nm)	r (nm)
25	8.4915×10^{-15}	2.35	3.58
40	8.4793×10^{-15}	2.35	3.66
59	8.4920×10^{-15}	2.35	3.78

3.6. Effect of ultrasound irradiation on the conformation

The above results revealed that the interaction did happen between ECG and BSA in the model wine, and ultrasonic irradiation did have effects on the binding interaction. In order to investigate the specific mechanism between them, experiments on conformation were performed to study the changes by three spectroscopic methods.

3.6.1. UV–Vis spectra

Spectroscopy is a common and qualitative method to observe conformational changes in proteins, since it allows non-invasive measurements of substances with lower concentration under mild conditions [29]. As shown in Fig. 4, the spectrum of BSA has two typical absorption peaks, the stronger peak at 215 nm accounts for the peptide bonds in the protein, and the weaker one at about 279 nm reflects the aromatic amino acid (Trp, Tyr, and Phe) [41]. With the addition of ECG, the peak intensity of BSA at 215 nm declined with a slight bathochromic shift (from 215 nm to 217 nm), and the peak at 279 nm had a very small decrease without obvious shift. These results indicated the formation of a complex between ECG and BSA in the model wine, confirming the static quenching. Furthermore, the red shift for the peak could be attributed to the loosening and unfolding of the protein skeleton, hence increasing the stability of the complex. As for the ultrasonic effect on the UV–Vis spectra, however, it is hard to differentiate the

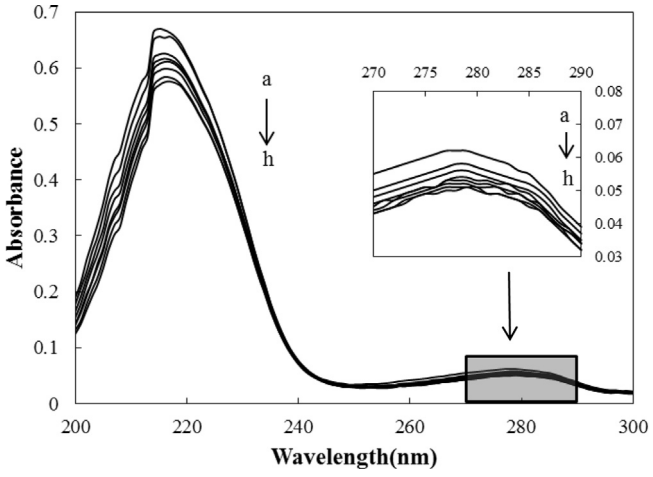

Fig. 4. UV–Vis spectra of BSA (1.0×10^{-6} mol·L^{-1}) in the presence of different concentrations of ECG (a–h: 0, 0.5, 1.0, 1.5, 2.0, 2.5, 3.0 and 3.5, 10^{-6} mol·L^{-1}) at 298 K and pH = 3.8.

spectra obtained without ultrasound irradiation from those obtained by ultrasound at different frequencies (data not shown) due to the limitation of sensitivity of this method.

3.6.2. Synchronous fluorescence

Synchronous fluorescence spectroscopy is one of the most commonly used methods to study the conformation of proteins, which can provide the characteristic information about molecular environment in the vicinity of fluorophores, such as tryptophan (Trp) and tyrosine (Tyr), and have several advantages, such as spectral simplification, reduction of the spectral bandwidth and avoidance of different perturbing effects [33]. Therefore, simultaneous scanning of the excitation and emission monochromators was performed to obtain the synchronous fluorescence spectra while maintaining a constant interval wavelength ($\Delta\lambda$) between them. The characteristic information of Tyr and Trp residues derived from synchronous fluorescence can be conveyed when the $\Delta\lambda$ is set at 15 nm and 60 nm, respectively.

It can be observed from Fig. 5 that the emission strengths of both Trp and Tyr residues decreased with the addition of ECG, and maximum emission wavelength of Trp and Tyr showed a slight red shift in all studied conditions. This phenomenon indicates that the polarity in the vicinity of Trp and Tyr residues was slightly increased, and therefore the hydrophobicity decreased around the residues in the presence of ECG. As for the effects of ultrasonic irradiation on the synchronous fluorescence spectra, it is apparent from Fig. 5c and d that the emission strengths of the samples exposed to ultrasound at 25 kHz decreased much more than those of untreated ones (Fig. 5a and b). Furthermore, as the ultrasonic frequency increases, the extent of emission strengths decrease presented a declining trend, and the phenomenons of red shift for the residues are similar in all conditions (data not shown). Overall, it can be inferred that regular conformational changes may occur with the ultrasonic frequency variation which could explain the regular change of the above mentioned binding parameters and critical distance from one side, whereas, meanwhile, ultrasound may only have few minor effects on the polarity of microenvironment around Trp and Tyr residues.

3.6.3. CD spectra

CD is a sensitive technique to observe the secondary structural changes of proteins, in order to further investigate the conformational changes induced by ultrasonic irradiation, the CD spectra of BSA and ECG-BSA complex in the absence and presence of ultrasonic treatment were measured in the range of 200 nm to 260 nm.

Two negative bands in the far UV regions at 208 nm and 222 nm can be observed in Fig. 6, which is indicative of α-helix for proteins [42]. There was a slight decrease of the values in both of these bands when higher ultrasound frequency was adopted for the model wine, which may indicate regular changes in the secondary structure of both free BSA and the complex. The secondary structure information was calculated and listed in Table 4 about the free BSA and the ECG-BSA complex affected by different ultrasound frequencies. It is apparent from Table 4 that, with the ultrasonic frequency increasing from 0 kHz to 59 kHz, the α-helix ratio of the ECG-BSA complex increased from 66.90% to 74.90%, along with a slight reduction in β-turn, parallel, antiparallel and random coil, which indicates a slight secondary conformation change of the complex. This phenomenon may be attributed to the changes of force acting within the complex, such as the hydrophobic interaction and hydrogen bond which could be interfered or disrupted by the quicker nonlinear oscillation of the cavitation bubbles combined with the more frequent pulses of the local instant high temperature (>5000 °C) and pressure (>1000 atm) with ultrasonic

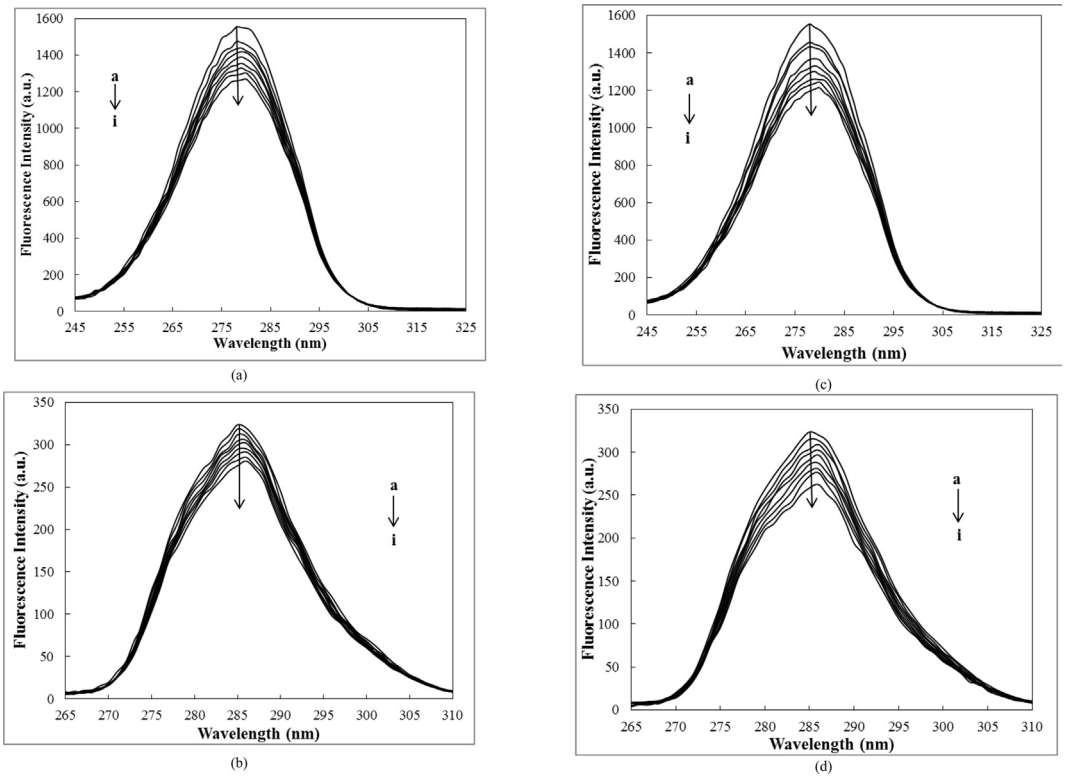

Fig. 5. Synchronous fluorescence spectra of BSA (1.0×10^{-6} mol·L^{-1}) in the presence of different concentrations of ECG (a–i: 0, 0.5, 1.0, 1.5, 2.0, 2.5, 3.0, 3.5 and 4.0, 10^{-6} mol·L^{-1}) at 298 K, and pH = 3.8. (a) $\Delta\lambda$ = 60 nm without ultrasound irradiation; (b) $\Delta\lambda$ = 15 nm without ultrasound irradiation; (c) $\Delta\lambda$ = 60 nm with ultrasound irradiation at 25 kHz, 500 W and 30 min; (d) $\Delta\lambda$ = 15 nm with ultrasound irradiation at 25 kHz, 500 W and 30 min.

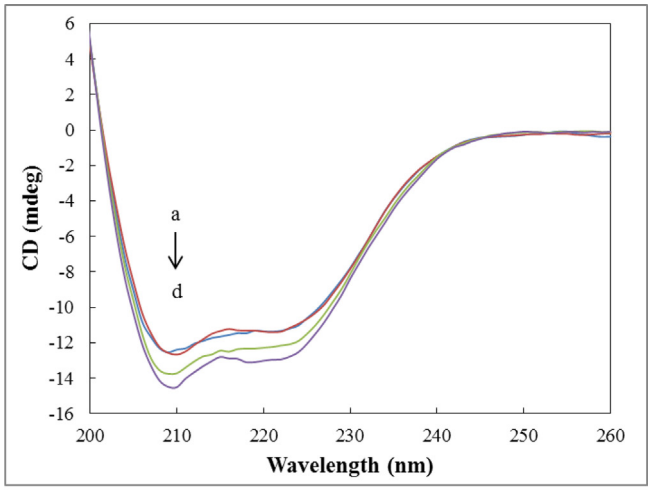

(a)

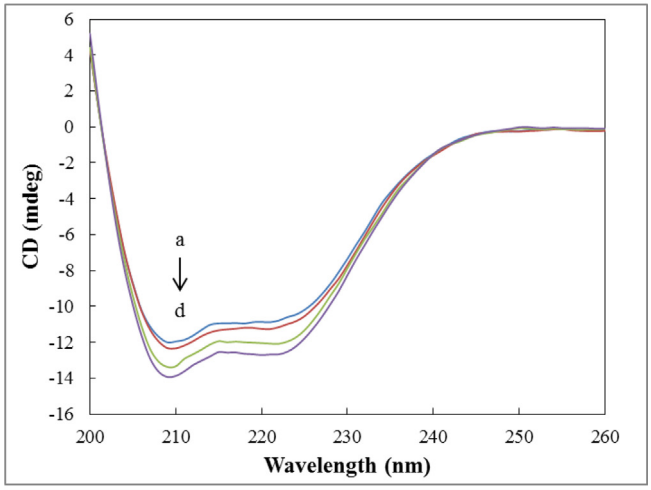

(b)

Fig. 6. CD spectra of ECG-BSA complex (a) or BSA (b) induced by ultrasonic treatment with different frequencies at 298 K in the model wine. Conditions: c (BSA) = 1.0×10^{-6} mol·L^{-1}, c(ECG) = 2.0×10^{-6} mol·L^{-1}, ultrasonic frequencies/kHz, a–d: 0, 25, 40 and 59, respectively.

frequency increasing. Apart from the above reasons, higher frequency may result in quicker shift or alternation between the rarefaction cycle and compression cycle, during which the collapse of bubbles occurs more rapidly, generating a higher amount of cavitation bubbles and subsequently releasing more hydrogen and oxygen radicals from bubbles to the model wine. Therefore, these free radicals may attack the covalent bonds in the BSA resulting in conformational change of the protein. Furthermore, compared with the data obtained from the samples of complex without ultrasonic irradiation, the secondary structural variation of the complex with ultrasound of 25 kHz is extremely limited, which may account for the relatively larger binding constant and shorter critical distance. Furthermore, as shown in Fig. 6b and Table 4, a similar variation trend for BSA can be observed which was solely exposed to ultrasound with different ultrasonic frequencies, indicating that ultrasound would have a regular effect on the secondary structure of BSA and, therefore, influence the affinity of BSA to ECG, which is consistent with the results derived from the synchronous fluorescence study. Considering the relatively limited influence of ultrasonic irradiation on the ECG in the experimental condition (data not shown), the structural change of BSA induced by ultrasonic treatment would play a major role in the ultrasonic modification of the interaction.

4. Conclusions

As discussed above, the binding interaction between ECG and BSA in the model wine was definitely influenced by the ultrasonic irradiation. From the binding parameters, the increase of ultrasonic frequency resulted in a decrease of binding stability, and could enlarge the distance between the fluorophore of BSA and ECG, as proved by the binding parameters. However, compared with the model wine untreated with ultrasound, it should be highlighted that the sample exposed to ultrasound of 25 kHz possessed a larger binding constant and shorter critical distance, which might indicate that the binding interaction could be promoted by the ultrasonic treatment. Furthermore, a regular conformational change was observed after ultrasound irradiation of different frequency, which might account for the change of the binding interaction induced by ultrasound. Overall, these results suggest that ultrasonic treatment at lower frequency might be a potential and simple technique to facilitate the interaction between proteins and phenols in wine during aging process, thus modifying the organoleptic property of wine. Nevertheless, the effect of other parameters of ultrasound irradiation on the binding interaction should be further studied in the future, such as ultrasound power and ultrasound time. In summary, these results do contribute to understand the mechanism of ultrasonic irradiation on modification of some wines and produce high quality wine with this novel technique in winery.

Acknowledgments

This study was funded by National Natural Science Foundation of China [No. 31101324], Natural Science Foundation of Shaanxi Province, China [No. 2015JM3097], the Fundamental Research Funds for the Central Universities of China [No. GK201602005].

Table 4
Percentage of secondary structure of the free BSA and its ECG complex with and without ultrasonic treatment in the model wine system.

	Frequency	0 kHz	25 kHz	40 kHz	59 kHz
c(ECG) = 0	α-Helix,%	63.65 ± 0.53^{a}	64.80 ± 0.30^{b}	70.73 ± 1.05^{c}	74.03 ± 0.94^{d}
	Antiparallel,%	3.25 ± 0.04^{a}	3.15 ± 0.05^{a}	2.53 ± 0.13^{a}	2.20 ± 0.08^{a}
	Parallel,%	3.55 ± 0.04^{a}	3.45 ± 0.05^{a}	2.80 ± 0.10^{a}	2.50 ± 0.08^{a}
	β-Turn,%	12.50 ± 0.07^{a}	12.25 ± 0.05^{a}	11.50 ± 0.15^{ab}	11.03 ± 0.12^{b}
	Random coil,%	15.70 ± 0.21^{a}	15.40 ± 0.10^{a}	12.93 ± 0.37^{b}	11.50 ± 0.33^{c}
c(ECG) = 2×10^{-6} mol L^{-1}	α-Helix,%	66.90 ± 0.07^{a}	66.90 ± 0.70^{a}	72.10 ± 0.37^{b}	74.90 ± 0.23^{c}
	Antiparallel,%	2.90 ± 0.00^{a}	2.90 ± 0.11^{a}	2.37 ± 0.05^{b}	2.10 ± 0.02^{c}
	Parallel,%	3.20 ± 0.00^{a}	3.20 ± 0.07^{a}	2.67 ± 0.05^{b}	2.40 ± 0.02^{c}
	β-Turn,%	12.00 ± 0.00^{a}	12.00 ± 0.12^{a}	11.30 ± 0.08^{b}	10.90 ± 0.04^{c}
	Random coil,%	14.20 ± 0.21^{a}	14.50 ± 0.21^{b}	12.30 ± 0.14^{c}	11.30 ± 0.16^{d}

Appendix A. Supplementary data

Supplementary data associated with this article can be found, in the online version, at http://dx.doi.org/10.1016/j.ultsonch.2017.01.031.

References

[1] Q.A. Zhang, Y. Shen, X.H. Fan, J.F. García Martín, Preliminary study of the effect of ultrasound on physicochemical properties of red wine, CyTA – J. Food 14 (2016) 55–64.
[2] Q.A. Zhang, Y. Shen, X.H. Fan, Y.Y. Yan, J.F. García Martín, Online monitoring of electrical conductivity of wine induced by ultrasound, CyTA – J. Food 14 (2015) 496–501.
[3] R. Brouillard, F. George, A. Fougerousse, Polyphenols produced during red wine ageing, BioFactors 6 (1997) 403–410.
[4] A.L. Waterhouse, V.F. Laurie, Oxidation of wine phenolics: a critical evaluation and hypotheses, Am. J. Enol. Vitic. 57 (2006) 306–313.
[5] H. Li, A. Guo, H. Wang, Mechanisms of oxidative browning of wine, Food Chem. 108 (2008) 1–13.
[6] G.B. Michèle, C. David, Comparison of components released by fermented or active dried yeasts after aging on lees in a model wine, J. Agri. Food Chem. 51 (2003) 746–751.
[7] A.J. Martínez-Rodríguez, M.C. Polo, Characterization of the nitrogen compounds released during yeast autolysis in a model wine system, J. Agri. Food Chem. 48 (2000) 1081–1085.
[8] J.F. García Martín, L. Guillemet, C. Feng, D.W. Sun, Cell viability and proteins release during ultrasound-assisted yeast lysis of light lees in model wine, Food Chem. 141 (2013) 934–939.
[9] M. Moutounet, V. Cheynier, T. Doco, P. Vuchot, Structural modification of wine arabinogalactans during aging on lees, Am. J. Enol. Vitic. 543 (2002) 150–157.
[10] J.M. Salmon, C. Fornairon-Bonnefond, J.P. Mazauric, Interactions between wine lees and polyphenols: influence on oxygen consumption capacity during simulation of wine aging, J. Food Sci. 67 (2006) 1604–1609.
[11] J.A. Pérez-Serradilla, M.D.L.d. Castro, Role of lees in wine production: a review, Food Chem. 111 (2008) 447–456.
[12] J.M. Nguela, C. Poncet-Legrand, N. Sieczkowski, A. Vernhet, Interactions of grape tannins and wine polyphenols with a yeast protein extract, mannoproteins and β-glucan, Food Chem. 210 (2016) 671–682.
[13] J.-P. Mazauric, J.-M. Salmon, Interactions between yeast lees and wine polyphenols during simulation of wine aging: I. Analysis of remnant polyphenolic compounds in the resulting wines, J. Agri. Food Chem. 53 (2005) 5647–5653.
[14] J.-P. Mazauric, J.-M. Salmon, Interactions between yeast lees and wine polyphenols during simulation of wine aging. II. Analysis of desorbed polyphenol compounds from yeast lees, J. Agri. Food Chem. 54 (2006) 3876–3881.
[15] S. Vidal, L. Francis, P. Williams, M. Kwiatkowski, R. Gawel, V. Cheynier, E. Waters, The mouth-feel properties of polysaccharides and anthocyanins in a wine like medium, Food Chem. 85 (2004) 519–525.
[16] C. Fornairon-Bonnefond, C. Camarasa, M. Moutounet, J.M. Salmon, New trends on yeast autolysis and wine ageing on lees: a bibliographic review, J. Int. Des Sci. De La Vigne Et Du Vin 36 (2002) 49–69.
[17] L. Martínez-Lapuente, Z. Guadalupe, B. Ayestarán, S. Pérez-Magariño, Role of major wine constituents in the foam properties of white and rosé sparkling wines, Food Chem. 174 (2015) 330–338.
[18] J.F. García Martín, D.W. Sun, Ultrasound and electric fields as novel techniques for assisting the wine ageing process: the state-of-the-art research, Trends Food Sci. Technol. 33 (2013) 40–53.
[19] T. Yang, J.F. García Martín, D.-W. Sun, Advances in wine aging technologies for enhancing wine quality and accelerating wine aging process, Crit. Rev. Food Sci. Nutr. 54 (2014) 817–835.
[20] H. Kiani, Z. Zhang, A. Delgado, D.W. Sun, Ultrasound assisted nucleation of some liquid and solid model foods during freezing, Food Res. Int. 44 (2011) 2915–2921.
[21] A.E. Delgado, L. Zheng, D.W. Sun, Influence of ultrasound on freezing rate of immersion-frozen apples, Food Bioprocess Technol. 2 (2009) 263–270.
[22] H. Kiani, D.W. Sun, A. Delgado, Z. Zhang, Investigation of the effect of power ultrasound on the nucleation of water during freezing of agar gel samples in tubing vials, Ultrason. Sonochem. 19 (2011) 576–581.
[23] A.C. Chang, F.C. Chen, The application of 20 kHz ultrasonic waves to accelerate the aging of different wines, Food Chem. 79 (2002) 501–506.
[24] A.C. Chang, Study of ultrasonic wave treatments for accelerating the aging process in a rice alcoholic beverage, Food Chem. 92 (2005) 337–342.
[25] N. Masuzawa, E. Ohdaira, M. Ide, Effects of ultrasonic irradiation on phenolic compounds in wine, Jpn. J. Appl. Phys. 39 (2000) 2978–2979.
[26] Q.A. Zhang, Y. Shen, X.H. Fan, J.F. García Martín, X. Wang, Y. Song, Free radical generation induced by ultrasound in red wine and model wine: an EPR spin-trapping study, Ultrason. Sonochem. 27 (2015) 96–101.
[27] Q.A. Zhang, H. Shen, X.H. Fan, S. Yuan, X. Wang, Y. Song, Changes of gallic acid mediated by ultrasound in a model extraction solution, Ultrason. Sonochem. 22 (2014) 149–154.
[28] X. Li, Y. Hao, Probing the binding of (+)-catechin to bovine serum albumin by isothermal titration calorimetry and spectroscopic techniques, J. Mol. Struct. 1091 (2015) 109–117.
[29] Y.J. Hu, Y. Liu, R.M. Zhao, J.X. Dong, S.S. Qu, Spectroscopic studies on the interaction between methylene blue and bovine serum albumin, J. Photochem. Photobiol., A 179 (2006) 324–329.
[30] S. Soares, N. Mateus, V.D. Freitas, Interaction of different polyphenols with bovine serum albumin (BSA) and human salivary α-amylase (HSA) by fluorescence quenching, J. Agri. Food Chem. 55 (2007) 6726–6735.
[31] J.R. Lakowicz, Principles of Fluorescence Spectroscopy Second, Edition ed., Kluwer Academic/Plenum Publishers, New York, Boston, Dordrecht, London, Moscow, 1999.
[32] A. Bose, Interaction of tea polyphenols with serum albumins: a fluorescence spectroscopic analysis, J. Lumin. 169 (2015) 220–226.
[33] P. Qin, R. Liu, X. Pan, X. Fang, Y. Mou, Impact of carbon chain length on binding of perfluoroalkyl acids to bovine serum albumin determined by spectroscopic methods, J. Agri. Food Chem. 58 (2010) 5561–5567.
[34] X. Yu, B. Jiang, Z. Liao, Y. Jiao, P. Yi, Study on the interaction between Besifloxacin and bovine serum albumin by spectroscopic techniques, Spectrochim. Acta Part A Mol. Biomol. Spectrosc. 149 (2015) 116–121.
[35] H. Lin, J. Lan, M. Guan, F. Sheng, H. Zhang, Spectroscopic investigation of interaction between mangiferin and bovine serum albumin, Spectrochim. Acta Part A Mol. Biomol. Spectrosc. 73 (2009) 936–941.
[36] W. Alfred, Biochemical effects of ultrasound: destruction of tryptophan, J. Acoust. Soc. Am. 32 (1960) 1499–1500.
[37] O.K. Abou-Zied, O.I. Al-Shihi, Characterization of subdomain IIA binding site of human serum albumin in its native, unfolded, and refolded states using small molecular probes, J. Am. Chem. Soc. 130 (2008) 10793–10801.
[38] S. Pal, C. Saha, M. Hossain, S.K. Dey, G.S. Kumar, Influence of galloyl moiety in interaction of epicatechin with bovine serum albumin: a spectroscopic and thermodynamic characterization, PLoS ONE 7 (2012) e43321.
[39] P.D. Ross, S. Subramanian, Thermodynamics of protein association reactions: forces contributing to stability, Biochemistry 20 (1981) 3096–3102.
[40] X. Zheng, M. Zhang, Z. Fang, Y. Liu, Effects of low frequency ultrasonic treatment on the maturation of steeped greengage wine, Food Chem. 162 (2014) 264–269.
[41] X. Zhao, R. Liu, Z. Chi, Y. Teng, P. Qin, New insights into the behavior of bovine serum albumin adsorbed onto carbon nanotubes: comprehensive spectroscopic studies, J. Phys. Chem. B 114 (2010) 5625–5631.
[42] D. Li, Y. Wang, J. Chen, B. Ji, Characterization of the interaction between farrerol and bovine serum albumin by fluorescence and circular dichroism, Bacteriol. Rev. 79 (2011) 680–686.